JACS
JOURNAL OF THE AMERICAN CHEMICAL SOCIETY

Communication

pubs.acs.org/JACS

Membrane-Permeable Mn(III) Complexes for Molecular Magnetic Resonance Imaging of Intracellular Targets

Ali Barandov,[†,∥] Benjamin B. Bartelle,[†,∥] Beatriz A. Gonzalez,[†] William L. White,[†] Stephen J. Lippard,[‡] and Alan Jasanoff*[,†,§,⊥]

Departments of [†]Biological Engineering, [‡]Chemistry, [§]Brain and Cognitive Sciences, and [⊥]Nuclear Science and Engineering, Massachusetts Institute of Technology, 77 Massachusetts Avenue, Cambridge, Massachusetts 02139, United States

Supporting Information

ABSTRACT: Intracellular compartments make up roughly two-thirds of the body, but delivery of molecular imaging probes to these spaces can be challenging. This situation is particularly true for probes designed for detection by magnetic resonance imaging (MRI), a high-resolution but relatively insensitive modality. Most MRI contrast agents are polar and membrane impermeant, making it difficult to deliver them in sufficient quantities for measurement of intracellular analytes. Here we address this problem by introducing a new class of planar tetradentate Mn(III) chelates assembled from a 1,2-phenylenediamido (PDA) backbone. Mn(III)-PDA complexes display T_1 relaxivity comparable to that of Gd(III)-based contrast agents and undergo spontaneous cytosolic localization via defined mechanisms. Probe variants incorporating enzyme-cleavable acetomethoxy ester groups are processed by intracellular esterases and accumulate in cells. Probes modified with ethyl esters preferentially label genetically modified cells that express a substrate-selective esterase. In each case, the contrast agents gives rise to robust T_1-weighted MRI enhancements, providing precedents for the detection of intracellular targets by Mn(III)-PDA complexes. These compounds therefore constitute a platform from which to develop reagents for molecular MRI of diverse processes inside cells.

The ability to map intracellular processes in space and time by non-invasive molecular imaging is highly desirable for studying organismic-level phenomena in the laboratory and clinic. MRI provides a combination of high spatiotemporal resolution and unlimited tissue penetration that makes it an ideal platform for application of cytosolic imaging probes, but few such probes currently exist. Most MRI contrast agents are complexes of Mn(II) or Gd(III) with aminopolycarboxylic acid chelating ligands that stabilize bound ions and reduce toxicity, but inherently limit membrane permeability. Nanoparticle-based MRI probes are more potent than paramagnetic complexes but, because of their size, are even less likely to permeate membranes.

Strategies to deliver MRI agents to cells have therefore made use of cell-permeable carrier vehicles,[1,2] but contrast agents delivered using such methods do not necessarily localize to the cytosol, limiting applicability for molecular imaging of many intracellular targets. A further strategy has been to shuttle agents into cells via active transport mechanisms under genetic control.[3−5] This task requires genetic manipulation of the recipient cell and so far has proved effective for delivery of relatively few probes. Additional receptor-targeting approaches are suitable for promoting cell uptake of MRI contrast agents, but not cytosolic probe localization.[6,7]

A mechanistically simpler strategy that could enable efficient delivery of intracellular molecular imaging agents is to design probes around paramagnetic platforms that are intrinsically membrane permeable.[8,9] To implement such a strategy, we prepared complexes of Mn(III) with tetradentate N_2O_2 and N_3O ligand systems derived from 1,2-phenylenediamine (PDA).[10,11] These ligands convey significant stability and magnetic properties of Mn(III) complexes arising from their high-spin d^4 electronic configurations, but they have not previously been explored as MRI contrast agents. Based on the structures of homologous compounds, Mn(III)-PDA complexes are likely to accommodate one or more exchangeable inner-sphere solvent or co-ligand molecules,[11,12] an ideal characteristic for T_1-weighted MRI contrast agents. These complexes differ from open-chain Mn-based MRI agents, which incorporate Mn(II) in d^5 configuration, requiring ligands with greater denticity to achieve thermodynamic and kinetic stabilization.[13] In Mn(III)-PDA complexes, we expect the combination of a lipophilic aryl backbone with a hydrophilic metal-binding site to afford a balance that facilitates crossing of cell membranes. PDA ligands should also provide greater rigidity than ethylenediamino ligands, and they are more stable to hydrolysis than *o*-phenylenediimine derivatives.[14]

Candidate PDA ligands **L1**−**L3** and their corresponding Mn complexes (Figure 1a) were synthesized as described in the Supporting Information. Spectra of the ligands and their complexes are presented in Figure S1. The absorbance signatures were used to measure Mn^{3+} dissociation constants of 1.2 ± 0.1 μM for **L1**, 610 ± 110 nM for **L2**, and 500 ± 80 nM for **L3** by titration with $Mn(OAc)_3$ (Figure S2). These values are inferior to the stabilities of commercial Gd-based MRI agents but comparable to those of the clinically approved Mn(II) agent Mn-*N*,*N*′-dipyridoxylethylenediamine-*N*,*N*′-diacetate 5,5′-bis(phosphate).[15] Octanol−water partition coefficients ($P_{oct/wat}$)[16] and solubilities of the three Mn-PDA complexes are presented in Table S1. The neutral Mn(III) complex Mn**L3** displays the highest lipophilicity, but all

Received: December 21, 2015

ACS Publications © XXXX American Chemical Society

DOI: 10.1021/jacs.5b13337
J. Am. Chem. Soc. XXXX, XXX, XXX−XXX

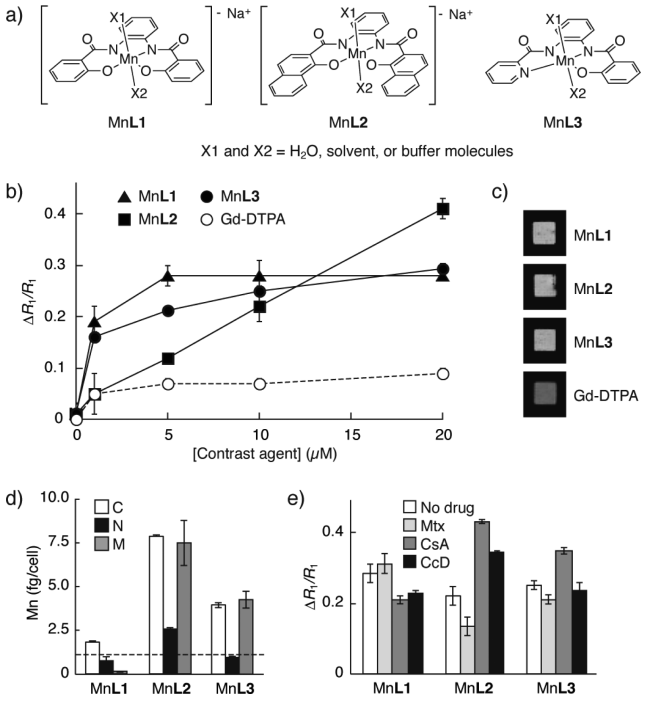

Figure 1. Cell-permeable Mn-PDA contrast agents. (a) Structures of three Mn-PDA complexes. (b) Relative change in T_1 relaxation rates ($\Delta R_1/R_1$) measured from HEK293 cells incubated with Mn**L1**−**L3** or with Gd-DTPA. (c) Images of cell pellets corresponding to the 10 μM incubation condition in (b). (d) Mn quantification by ICP-MS in cytosolic (C), nuclear (N), and membranous (M) fractions obtained from cells incubated with 10 μM Mn**L1**−**L3**. Horizontal line indicates cytosolic Mn quantified from unlabeled cells. (e) Effects of treatment with 50 μM Mtx, 20 μM CsA, or 5 μM CcD on cell labeling by 10 μM Mn**L1**−**L3**. Error bars denote SD, $n \geq 3$.

complexes have higher log $P_{oct/wat}$ values than the clinical contrast agent Gd-diethylaminetriamine pentaacetic acid (DTPA). The T_1 relaxivity (r_1) of each complex, a measure of its strength as an MRI contrast agent, was determined at 7 T and 22 °C. Values of r_1 for Mn**L1**, Mn**L2**, and Mn**L3** are 4.1 ± 0.1, 5.4 ± 0.2, and 5.1 ± 0.1 mM^{-1} s^{-1}, respectively, comparable to that of Gd-DTPA.[17] Relaxivity values were also determined at 3 T (Table S1), and for Mn**L3** at 7 T, in the presence of serum albumin, bicarbonate, and phosphate (Table S2). These measurements indicate that Mn-PDA agents combine robust performance as contrast agents with physicochemical properties conducive to membrane permeability.

To assess the cell-labeling characteristics of the new contrast agents, HEK293 cells were incubated with up to 20 μM of the Mn-PDA compounds for 30 min, followed by washing and then MRI analysis. Negligible toxicity was observed under these conditions (Figure S3). All three Mn-PDA agents appeared to label cells readily, producing enhancements of 28% ± 3%, 41% ± 4%, and 29% ± 1% in the T_1 relaxation rates (R_1) measured from cells incubated with 20 μM Mn**L1**, Mn**L2**, and Mn**L3**, respectively (Figure 1b). These changes reflect substantial T_1-weighted contrast enhancements observed in cell pellet images (Figure 1c). The more hydrophilic Gd-DTPA produced smaller R_1 changes with minimal visible contrast, and the cell-permeable ion Mn^{2+} produced a concentration-dependent labeling profile similar to that of Mn**L3** (Figure S4).

To explain the enhancements in cell pellet R_1 in terms of subcellular localization patterns, cells were fractionated after 30 min labeling with 10 μM of each of the contrast agents. These extracts were analyzed by inductively coupled plasma mass spectrometry (ICP-MS). Total manganese levels of 2.62 ± 0.05, 18.3 ± 1.2, and 9.3 ± 0.8 fg/cell were observed among fractions labeled with Mn**L1**, Mn**L2**, and Mn**L3**, respectively. Fractionation results (Figure 1d) indicated that both Mn**L2** and Mn**L3** display strong cytosolic localization combined with roughly equal membranous concentrations, consistent with their hydrophobicity. In contrast, Mn**L1** shows considerably lower cytosolic localization, and negligible levels in membranous fractions. The findings thus indicate that Mn**L2** and Mn**L3** penetrate cells more effectively than Mn**L1**. The fact that Mn**L1** gives rise to R_1 enhancements comparable to those found with Mn**L2** and Mn**L3** argues that Mn**L1** may have higher cell-associated r_1, or that it could be bound to the cell exterior and partially lost during fractionation. The second explanation is supported by ICP-MS analysis of minimally treated cell pellets, which shows ∼30% more total Mn in Mn**L1**-treated cells than in those prepared with Mn**L3**.

To probe the contributions of selected active import or export mechanisms to cell labeling by the Mn-PDA complexes, we repeated the cell labeling studies of Figure 1b in the presence of methotrexate (Mtx), which inhibits import of compounds by folate transporters RFC1 and PCFT, and cyclosporin A (CsA), which blocks compound export via the multidrug resistance protein MDR1; both the folate and multidrug transport pathways have been specifically shown to process planar aromatic compounds similar to our Mn-PDA complexes.[18,19] We also tested the affects of cytochalasin D (CcD), which blocks actin polymerization required for endocytosis. Results summarized in Figures 1e and S5 indicate that Mn**L2** cell labeling is significantly affected by all three drugs (*t*-test $p < 0.006$, $n = 3$), indicating susceptibility of Mn**L2** to active transport mechanisms, despite its apparently non-saturating labeling profile in Figure 1b. In contrast, Mn**L3** cell labeling is enhanced by CsA ($p = 0.008$) but unaffected by Mtx or CcD ($p > 0.1$). Mn**L1** labels cells somewhat more poorly in the presence of CsA and CcD. The fact that cell labeling by Mn**L2** and Mn**L3**, but not Mn**L1**, is promoted by CsA supports evidence that these two compounds localize more effectively to the cytosol, where MDR1 is active.

The cell labeling and fractionation studies show that Mn**L3** displays the clearest evidence of innate membrane permeability of the three Mn-PDA agents, consistent with its lipophilicity. Tests of resistance to dissociation (Figure S6) and transmetalation (Figure S7) revealed the stability of this compound in the presence of excess ethylenediaminetetraacetic acid (EDTA) and biologically relevant transition metals for up to 48 h. Based on these results and its other properties, Mn**L3** was deemed most suitable as a platform for development of further membrane-permeant agents.

We next sought to determine whether Mn**L3** could be incorporated into probes for MRI-based detection of intracellular species. Intracellular esterases represent an important class of targets for imaging agents that can reach the cell interior. Endogenous or ectopically expressed esterases can trap appropriately esterified probes.[20−22] Previous studies have introduced esterase-sensitive MRI contrast agents, but none has demonstrated intracellular cleavage or cytosolic trapping.[23−26] To test the ability of Mn**L3**-based **M**RI contrast agents to undergo esterase-dependent capture and accumulation in cells, we synthesized an acetoxymethyl (AM)-modified Mn**L3** analogue, Mn**L3-OAc-AM**. AM esters are well-known

DOI: 10.1021/jacs.5b13337
J. Am. Chem. Soc. XXXX, XXX, XXX−XXX

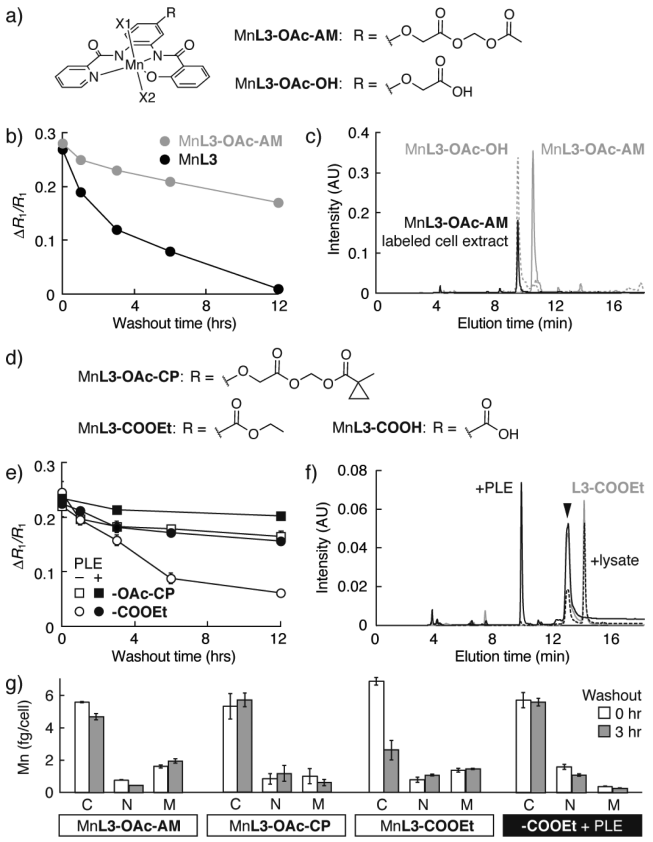

Figure 2. Targeting intracellular esterases with Mn-PDA contrast agents. (a) Esterase substrate Mn**L3-OAc-AM** and its hydrolysis product. (b) Washout time courses from cells pre-incubated with 10 μM Mn**L3-OAc-AM** or Mn**L3**. (c) HPLC analysis of extracts from cells labeled with Mn**L3-OAc-AM** (black). The elution peak corresponds to Mn**L3-OAc-OH** (dashed), rather than Mn**L3-OAc-AM** (solid gray), indicating complete hydrolysis in cells. (d) Side-chain structures of Mn**L3-OAc-CP**, Mn**L3-COOEt**, and Mn**L3-COOH**. (e) Washout time courses from cells incubated with 10 μM Mn**L3-OAc-CP** or Mn**L3-COOEt**, following transfection with genes encoding either PLE or green fluorescent protein. (f) HPLC traces obtained from 5 μM **L3-COOEt** alone (gray) and following treatment with cell lysate (black dotted) or 15 units PLE (solid line), showing selective cleavage. (g) Quantification of Mn in fractions from cells incubated with the agents, at washout times t = 0 and 3 h. All measurements $n \geq 3$; error bars denote SD.

substrates for intracellular esterases,[20] so we anticipated that Mn**L3-OAc-AM** would enter cells and be processed into a charged and membrane-impermeant product, Mn**L3-OAc-OH** (Figure 2a).

Cells were incubated for 30 min with 10 μM Mn**L3-OAc-AM** or with Mn**L3** control, rinsed, incubated for a variable wash-out delay period, rinsed again to remove extracellular contrast agent, and then imaged by MRI to measure contrast arising from remaining intracellular probe. Consistent with an esterase-mediated trapping mechanism, Mn**L3** and Mn**L3-OAc-AM** displayed striking differences in wash-out kinetics (Figure 2b). Cells incubated with each compound showed similar initial R_1 values, indicating equivalent labeling efficiency. Cells labeled with Mn**L3** displayed a complete return to baseline R_1 over 12 hrs, with a half-life of ~3 h. In contrast, cells pre-loaded with Mn**L3-OAc-AM** displayed only a 37% reduction in R_1 over 12 h, with a half-life longer than the experimental duration. Fractionation and analytical HPLC analysis of cells incubated with Mn**L3-OAc-AM** revealed complete conversion of this compound into the expected product Mn**L3-OAc-OH** (Figure 2c). These results confirm that complete hydrolysis of the esterase-targeted contrast agent Mn**L3-OAc-AM** takes place in labeled cells.

Given the evidence for endogenous esterase-mediated cell trapping of Mn**L3-OAc-AM**, we wondered whether selective esterase-mediated cell trapping[22] could be implemented as part of a strategy for genetically targeting Mn**L3** derivatives. Two candidates for selective esterase processing were therefore synthesized, one bearing a cyclopropyl ester moiety (Mn**L3-OAc-CP**) and the other bearing a simple ethyl ester (Mn**L3-COOEt**) (Figure 2d).

These further Mn**L3**-based esters were co-incubated with HEK293 cells transfected with constructs encoding either green fluorescent protein (GFP, control) or a porcine liver esterase (PLE) known to exhibit distinct specificity from the repertoire of esterases normally present in these cells.[22] As expected based on their similarity to Mn**L3-OAc-AM**, both Mn**L3-OAc-CP** and Mn**L3-COOEt** were effectively taken up by PLE-expressing cells as well as control cells, and neither showed evidence of acute cell toxicity (Figure S8). Retention of the contrast agents differed significantly, however. MRI results suggested that, although both Mn**L3-OAc-CP** and Mn**L3-COOEt** were retained in PLE-expressing cells, the ethyl ester Mn**L3-COOEt** showed substantially greater selectivity for PLE cells compared with control cells not transfected with the PLE gene (Figure 2e). After 12 h, the R_1 enhancement of cells incubated with Mn**L3-COOEt** was reduced by 75%, whereas the R_1 increase of cells loaded with Mn**L3-OAc-CP** was reduced by 32%, only 7% more than the reduction observed for Mn**L3-OAc-AM**.

The cell retention results suggest that Mn**L3-COOEt** is cleaved more effectively in the presence of expressed PLE than by endogenous intracellular esterases alone.[27] To evaluate this possibility, we monitored **L3-COOEt** in buffer following addition of 20 mg of HEK293 cell extract or 15 units of purified PLE. As predicted from the cell labeling MRI result, the contrast agent was hydrolyzed much more effectively in the presence of PLE (Figure 2f). In contrast, the **L3-OAc-CP** ligand was found to be hydrolyzed completely by addition of cell extract alone, with no requirement for PLE, explaining the non-specific retention of Mn**L3-OAc-CP** in untransfected cells (Figure S9). To obtain further evidence for the esterase specificity of these selective retention effects, we performed a fractionation and ICP-MS analysis of HEK293 cells incubated with 10 μM Mn**L3-OAc-AM**, Mn**L3-OAc-CP**, or Mn**L3-COOEt**, followed by either 0 or 3 h washout periods. Only Mn**L3-COOEt** showed substantial reduction in cytosolic content during this period, and this reduction was absent in cells expressing PLE.

Our data thus indicate that Mn-PDA agents have the ability to enter cells and interact with distinct cytosolic enzymes, demonstrating their suitability for molecular imaging of intracellular targets. The basic architecture of the Mn-PDA agents allows for facile synthesis, confers stability, and provides MRI T_1 relaxivity comparable to that of commercial contrast agents. Of the compounds surveyed, the neutral complex Mn**L3** seemed to be the best candidate for further modification. Functionalization of Mn**L3** with different ester groups did not diminish cell uptake, showing that Mn**L3** can indeed act as a building block for molecular imaging agents.

DOI: 10.1021/jacs.5b13337
J. Am. Chem. Soc. XXXX, XXX, XXX−XXX

Although we present Mn-PDA-based esterase substrates as a proof of concept for MRI detection of intracellular analytes, these contrast agents could also be used for molecular imaging themselves. In particular, ester derivatives of Mn**L3** are likely to be effective reagents for cell labeling and *in vivo* cell tracking. Specific labeling of cells expressing PLE or related enzymes could also provide a pathway to reporter gene mapping by MRI. Although extracellular esterases might interfere under some circumstances,[28] extracellularly hydrolyzed agents would not tend to be trapped, and therefore might not contribute heavily to background signal. Additional targeted or responsive agents could be constructed by modifying the Mn-PDA platform. This new family of contrast agents would be most applicable for molecular imaging applications in animals, but the stability and relaxivity of Mn-PDA derivatives might eventually enable applications in human subjects.

■ ASSOCIATED CONTENT

Supporting Information

The Supporting Information is available free of charge on the ACS Publications website at DOI: 10.1021/jacs.5b13337.

Detailed methods and further characterization of synthetic compounds, including Scheme S1, Figures S1−S9, and Tables S1 and S2 (PDF)

■ AUTHOR INFORMATION

Corresponding Author

*jasanoff@mit.edu

Author Contributions

‖A.B. and B.B.B. contributed equally.

Notes

The authors declare no competing financial interest.

■ ACKNOWLEDGMENTS

The authors thank Atushi Takahashi, Koli Taghizadeh, Emily Young, and Emily Loucks. Funding came from the MIT Simons Center and NIH grants R21-MH102470 and U01-NS090451 to A.J., as well as grant P30-ES002109 for the CEHS Bioanalytical Core.

■ REFERENCES

(1) Bhorade, R.; Weissleder, R.; Nakakoshi, T.; Moore, A.; Tung, C.-H. *Bioconjugate Chem.* **2000**, *11*, 301.

(2) Hung, A. H.; Holbrook, R. J.; Rotz, M. W.; Glasscock, C. J.; Mansukhani, N. D.; MacRenaris, K. W.; Manus, L. M.; Duch, M. C.; Dam, K. T.; Hersam, M. C.; Meade, T. J. *ACS Nano* **2014**, *8*, 10168.

(3) Weissleder, R.; Moore, A.; Mahmood, U.; Bhorade, R.; Benveniste, H.; Chiocca, E. A.; Basilion, J. P. *Nat. Med.* **2000**, *6*, 351.

(4) Bartelle, B. B.; Szulc, K. U.; Suero-Abreu, G. A.; Rodriguez, J. J.; Turnbull, D. H. *Magn. Reson. Med.* **2013**, *70*, 842.

(5) Patrick, P. S.; Hammersley, J.; Loizou, L.; Kettunen, M. I.; Rodrigues, T. B.; Hu, D.-E.; Tee, S.-S.; Hesketh, R.; Lyons, S. K.; Soloviev, D.; Lewis, D. Y.; Aime, S.; Fulton, S. M.; Brindle, K. M. *Proc. Natl. Acad. Sci. U. S. A.* **2014**, *111*, 415.

(6) Aime, S.; Barge, A.; Cabella, C.; Crich, S.; Gianolio, E. *Curr. Pharm. Biotechnol.* **2004**, *5*, 509−518.

(7) McCarthy, J. R.; Kelly, K. A.; Sun, E. Y.; Weissleder, R. *Nanomedicine* **2007**, *2*, 153.

(8) Lee, T.; Zhang, X.; Dhar, S.; Faas, H.; Lippard, S. J.; Jasanoff, A. *Chem. Biol.* **2010**, *17*, 665.

(9) Zhang, X.; Lovejoy, K. S.; Jasanoff, A.; Lippard, S. J. *Proc. Natl. Acad. Sci. U. S. A.* **2007**, *104*, 10780.

(10) Bertoncello, K.; Fallon, G. D.; Murray, K. S. *Inorg. Chim. Acta* **1990**, *174*, 57.

(11) Sunatsuki, Y.; Shimada, H.; Matsuo, T.; Nakamura, M.; Kai, F.; Matsumoto, N.; Re, N. *Inorg. Chem.* **1998**, *37*, 5566.

(12) Yang, C.; Wang, Q.-L.; Ma, Y.; Tang, G.-T.; Liao, D.-Z.; Yan, S.-P.; Yang, G.-M.; Cheng, P. *Inorg. Chem.* **2010**, *49*, 2047.

(13) Gale, E. M.; Atanasova, I. P.; Blasi, F.; Ay, I.; Caravan, P. *J. Am. Chem. Soc.* **2015**, *137*, 15548.

(14) Venkataramanan, N. S.; Kuppuraj, G.; Rajagopal, S. *Coord. Chem. Rev.* **2005**, *249*, 1249.

(15) Rocklage, S. M.; Cacheris, W. P.; Quay, S. C.; Hahn, F. E.; Raymond, K. N. *Inorg. Chem.* **1989**, *28*, 477.

(16) Leo, A.; Hansch, C.; Elkins, D. *Chem. Rev.* **1971**, *71*, 525.

(17) Shen, Y.; Goerner, F. L.; Snyder, C.; Morelli, J. N.; Hao, D.; Hu, D.; Li, X.; Runge, V. M. *Invest. Radiol.* **2015**, *50*, 330.

(18) Hou, Z.; Matherly, L. H. *Curr. Top. Membr.* **2014**, *73*, 175−204.

(19) Leslie, E. M.; Deeley, R. G.; Cole, S. P. C. *Toxicol. Appl. Pharmacol.* **2005**, *204*, 216.

(20) Tsien, R. Y. *Nature* **1981**, *290*, 527.

(21) Rehberg, M.; Lepier, A.; Solchenberger, B.; Osten, P.; Blum, R. *Cell Calcium* **2008**, *44*, 386.

(22) Tian, L.; Yang, Y.; Wysocki, L. M.; Arnold, A. C.; Hu, A.; Ravichandran, B.; Sternson, S. M.; Looger, L. L.; Lavis, L. D. *Proc. Natl. Acad. Sci. U. S. A.* **2012**, *109*, 4756.

(23) Himmelreich, U.; Aime, S.; Hieronymus, T.; Justicia, C.; Uggeri, F.; Zenke, M.; Hoehn, M. *NeuroImage* **2006**, *32*, 1142.

(24) Giardiello, M.; Lowe, M. P.; Botta, M. *Chem. Commun.* **2007**, 4044.

(25) Li, Y.; Sheth, V. R.; Liu, G.; Pagel, M. D. *Contrast Media Mol. Imaging* **2011**, *6*, 219.

(26) MacRenaris, K. W.; Ma, Z.; Krueger, R. L.; Carney, C. E.; Meade, T. J. *Bioconjugate Chem.* **2016**, *27*, 465.

(27) Lind, P. A.; Daniel, R. M.; Monk, C.; Dunn, R. V. *Biochim. Biophys. Acta, Proteins Proteomics* **2004**, *1702*, 103.

(28) Jobsis, P. D.; Rothstein, E. C.; Balaban, R. S. *J. Microsc.* **2007**, *226*, 74.

DOI: 10.1021/jacs.5b13337
J. Am. Chem. Soc. XXXX, XXX, XXX−XXX